

## Multi-objective control design for a truck cabin

Semiha Türkay\* Hüseyin Akçay \*\*

\*Department of Electrical and Electronics Engineering , Anadolu University,  
26555, Eskişehir, Turkey; (Tel: +90-222-3350580; e-mail:  
semihaturkay@anadolu.edu.tr)

\*\* Department of Electrical and Electronics Engineering , Anadolu University,  
26555 Eskişehir, Turkey; (e-mail: huakçay@anadolu.edu.tr)

---

**Abstract:** In this paper, a multi-objective control of a three-degrees-of-freedom cabin model for a commercial truck excited by random road disturbances is studied. The multi-objective control problem is formulated as a non-convex and non-smooth optimization problem with controller order restricted to be less than the vehicle model order. For a range of control orders, controllers are synthesized by using the HIFOO toolbox. The simulation results show that the cabin vibrations are effectively suppressed by this methodology.

---

### 1. INTRODUCTION

Heavy road vehicles are typically used for transportation and have different characteristics than those of a car. They may have more than two axles and each axle weighs an order of magnitude greater than a typical car axle. In addition, heavy vehicles comprise more than one unit and thus require distinct suspension design approaches. In the comprehensive work of Cole (2001), published literature on suspension design for heavy road vehicles was surveyed and fundamental issues in suspension design for heavy road vehicles that require further attention were identified.

The issue of ride comfort for vehicle operations has generated considerable interest recently; see for example Thomson (1971), Hrovat, (1993), Fialho and Balas (2002), Akçay and Türkay (2011). Since long-distance drivers are more likely to experience high levels of vibration it is an important factor in transportation and can be defined as how a vehicle responds to different road conditions or inputs. In order to capture, record and to analyze the ride vibration in practice, measuring sensors, i.e., ‘accelerometers’ are used.

Very few studies took an integrated look at the primary and secondary suspensions. In Uffelman (1993), elimination of the seat suspension and using softer cabin suspension and stiffer primary suspension was suggested. It was argued that the primary suspension dampers are not effective in dissipating the vibration energy due to the frame bending, and as a result, the driver can experience large levels of vibrations in the longitudinal and the vertical directions, depending on the cabin mounting and location. The cabin and the seat suspension system (secondary suspension) provides the driver with a comfortable ride without requiring soft primary suspension and consequent problems with vehicle handling, stability, and static deflection. Recent activity El Madany (1988), Tong et al. (1999), in the area of cabin and suspension design has focused on the use of controllable suspension elements which provide ride benefits of active/semi-active primary suspension.

In El Madany, (1988), stochastic optimal control theory was used to design an active cabin suspension for a tractor semi-trailer. A pitch-plane model, including the first bending modes of the frames, was used, and the control law was calculated for a range of vehicle speeds. Tong et al. (1999), proposed a design comprising semi-active cabin and seat suspensions on a tractor-semi-trailer. The suspension system consisted of semi-active dampers with sky-hook controllers, and the ride quality was assessed using a dynamic model of a cabin with two-degrees-of-freedom. The longitudinal and the pitch motions of the driver were not considered. The selected vehicle model was planar and included a cabin with two-degrees-of-freedom: the pitch and the vertical displacement.

A controller design method based on the modal input-output decoupling was proposed in Evers et al. (2009). Application of non-convex and non-smooth optimization algorithms in Overton, (2011) to suspension control problems was reported in the recent works Gümüşsoy et al. (2009), Akçay and Türkay (2011). Solutions to these problems were obtained by using the HIFOO toolbox and the results were compared with benchmarks in the literature.

The purpose of this study is to analyze the ride motions of the cabin under random excitations transmitted from the primary suspension and to improve the cabin ride performance by designing a suitable low order controller. The active suspension systems synthesized in Section 3 by using the HIFOO toolbox show that controllers with low-complexity, for example a static or first-order controllers yield remarkable performance improvements in heave, pitch and roll accelerations. It is unlikely to reach these performance levels with any other zeroth or first degrees-of-freedom controllers in the literature under the same complexity constraint, see for example Akçay and Türkay (2009).

The outline of the paper is as follows. A three-degrees-of-freedom cabin model for a mid-sized commercial truck is reviewed in Section 2 and in Section 3, a multi-objective

suspension control problem is formulated and solved by using HIFOO toolbox. The paper is concluded in Section 4.

## 2. THE THREE-DEGREES- OF-FREEDOM TRUCK CABIN MODEL

A three-degrees-of-freedom truck cabin model intended to study the heave, the pitch and the roll motions of the vehicle is shown in Figure 1. The displacements at the chassis points  $A'$ ,  $B'$ ,  $C'$ ,  $D'$  with respect to an inertial frame are denoted respectively by  $w_A, w_B, w_C, w_D$ . Let  $z_A, z_B, z_C, z_D$  denote the displacements at the corners  $a, b, c, d$  of the cabin with respect to this inertial frame. The cabin center of gravity, its mass, and the heave degree-of-freedom are denoted respectively by  $G, m_s$  and  $z_G$ . The pitch and the roll degrees-of-freedom and moments of inertia are denoted respectively by  $\theta, \phi, I_x$ , and  $I_y$ .

The cabin secondary suspension system consists of the actuators  $u_A, u_B, u_C, u_D$  in parallel with the linear passive

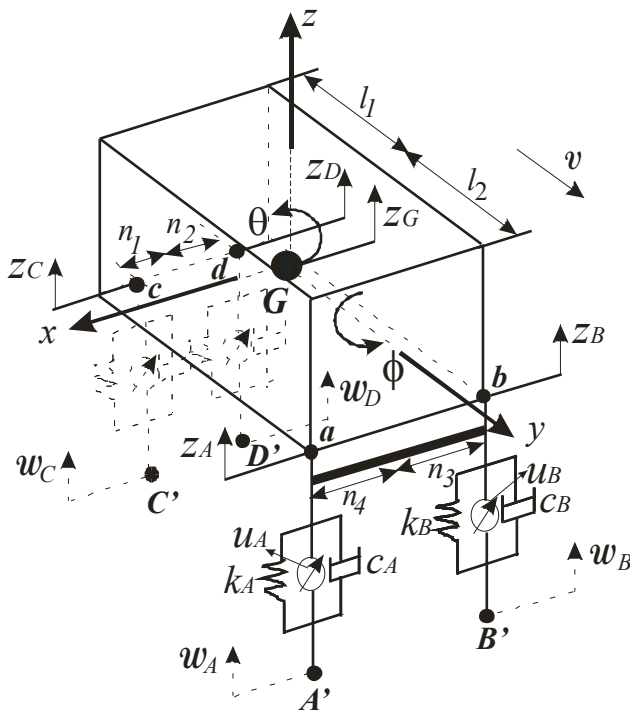


Fig. 1. Truck cabin model

suspension elements:  $k_A, k_B, k_C, k_D$  (the springs) and  $c_A, c_B, c_C, c_D$  (the dampers). At the front, an anti-roll bar denoted by  $K_F$  is included in the cabin model. The parameter values chosen for this study are typical for a mid-sized truck cabin and are summarized in Table 1. Assuming that small motions take place, the governing equations of motion are derived as follows:

$$\begin{aligned} z_A &= z_G + l_2 \theta - n_4 \phi \\ z_B &= z_G + l_2 \theta + n_3 \phi \\ z_C &= z_G - l_1 \theta - n_1 \phi \\ z_D &= z_G - l_1 \theta + n_2 \phi \end{aligned}$$

or compactly,

$$z_S = Sx_S$$

are easily derived where

$$S = \begin{bmatrix} 1 & l_2 & -n_4 \\ 1 & l_2 & n_3 \\ 1 & -l_1 & -n_1 \\ 1 & -l_1 & n_1 \end{bmatrix}$$

$$z_S = \begin{bmatrix} z_A \\ z_B \\ z_C \\ z_D \end{bmatrix}, \quad x_S = \begin{bmatrix} z_G \\ \theta \\ \phi \end{bmatrix}.$$

Let  $z_A - w_A$  and  $z_B - w_B$  denote the suspension strokes at the corners  $a$  and  $b$ . Then, the rotation of the anti-roll bar in the counter-clockwise direction is given by

Table 1. The vehicle parameters for the truck-cabin model.

Cabin mass	$m_c$	900 kg
Pitch moment of inertia	$I_x$	700 kg m <sup>2</sup>
Roll moment of inertia	$I_y$	650 kg m <sup>2</sup>
Front-right/left suspension stiffness	$k_A, k_B$	31,000 N/m
Rear-right/left suspension stiffness	$k_C, k_D$	15,500 N/m
Front-right/left damping coefficient	$c_A, c_B$	680 Ns/m
Rear-right/left damping coefficient	$c_C, c_D$	560 Ns/m
Front anti-roll bar stiffness	$K_F$	30,000 N/m
Distance between front-right/left corner and cabin c. g. along $x$ axis	$n_3, n_4$	0.84 m
Distance between rear-right/left corner and cabin c. g. along $x$ axis	$n_1, n_2$	0.68 m
Distance between front-right/left corner and cabin c. g. along $y$ axis	$l_2$	0.409 m
Distance between rear-right/left corner and cabin c. g. along $y$ axis	$l_1$	1.091 m

$$\phi_F = \frac{(z_A - w_A) - (z_B - w_B)}{n_3 + n_4}$$

and accordingly a pair of forces  $\pm f$  is formed as

$$f(n_3 + n_4) = K_F \phi_F,$$

or more explicitly,

$$f = K_F \frac{(z_A - w_A) - (z_A - w_B)}{(n_3 + n_4)^2}.$$

Now, let  $F_A, F_B, F_C, F_D$  denote respectively the forces at the corners  $a, b, c, d$  exerted by the suspension system. Then, the following relations hold for  $F_A, F_B, F_C, F_D$ :

$$F_A = -f - k_A(z_A - w_A) - c_A(\dot{z}_A - \dot{w}_A) - u_A,$$

$$F_B = f - k_B(z_B - w_B) - c_B(\dot{z}_B - \dot{w}_B) - u_B,$$

$$F_C = -k_C(z_C - w_C) - c_C(\dot{z}_C - \dot{w}_C) - u_C,$$

$$F_D = -k_D(z_D - w_D) - c_D(\dot{z}_D - \dot{w}_D) - u_D.$$

Thus,

$$m_c \ddot{z}_G = F_A + F_B + F_C + F_D,$$

$$I_x \ddot{\theta} = (F_A + F_B)l_2 - (F_C + F_D)l_1,$$

$$I_y \ddot{\phi} = -F_A n_4 + F_B n_3 - F_C n_1 + F_D n_2.$$

Setting,

$$w = \begin{bmatrix} w_A \\ w_B \\ w_C \\ w_D \end{bmatrix}, \quad u = \begin{bmatrix} u_A \\ u_B \\ u_C \\ u_D \end{bmatrix}, \quad \hat{z}_S = z_S - w,$$

the following equations of motion:

$$m_c \ddot{z}_G = -[k_A \quad k_B \quad k_C \quad k_D] \hat{z}_S - [c_A \quad c_B \quad c_C \quad c_D] \dot{\hat{z}}_S - [1 \quad 1 \quad 1 \quad 1]u$$

$$I_x \ddot{\theta} = -[k_A l_2 \quad k_B l_2 \quad -k_C l_1 \quad -k_D l_1] \hat{z}_S$$

$$- [c_A l_2 \quad c_B l_2 \quad -c_C l_1 \quad -c_D l_1] \dot{\hat{z}}_S$$

$$- [l_2 \quad l_2 \quad -l_1 \quad -l_1]u,$$

$$I_y \ddot{\phi} = [k_A n_4 + \frac{K_F}{n_3 + n_4} \quad - (k_B n_3 - \frac{K_F}{n_3 + n_4}) k_C n_1$$

$$- k_D n_2] \hat{z}_S + [c_A n_4 \quad -c_B n_3 \quad c_C n_1 - c_D n_2] \dot{\hat{z}}_S$$

$$+ [n_4 \quad -n_3 \quad n_1 \quad -n_2]u,$$

or more compactly,

$$M \ddot{x}_S + K \hat{z}_S + C \dot{\hat{z}}_S + W u = 0$$

are obtained where

$$M = \begin{bmatrix} m_c & 0 & 0 \\ 0 & I_x & 0 \\ 0 & 0 & I_y \end{bmatrix},$$

$$K = [K_1 \quad K_2],$$

$$K_1 = \begin{bmatrix} k_A & k_B \\ k_A l_2 & k_B l_2 \\ \left(-k_A n_4 - \frac{K_F}{n_3 + n_4}\right) & \left(k_B n_3 + \frac{K_F}{n_3 + n_4}\right) \end{bmatrix},$$

$$K_2 = \begin{bmatrix} k_C & k_D \\ -k_C l_1 & -k_D l_2 \\ -k_C n_1 & k_D n_2 \end{bmatrix},$$

$$C = \begin{bmatrix} c_A & c_B & c_C & c_D \\ c_A l_2 & c_B l_2 & -c_C l_1 & -c_D l_1 \\ -c_A n_4 & c_B n_3 & -c_C n_1 & c_D n_2 \end{bmatrix},$$

$$W = \begin{bmatrix} 1 & 1 & 1 & 1 \\ l_2 & l_2 & -l_1 & -l_1 \\ -n_4 & n_3 & -n_1 & n_2 \end{bmatrix}.$$

Then, from

$$\hat{z}_S = S x_S - w,$$

we get

$$M \ddot{x}_S + K S x_S - K w + C S \dot{x}_S - C \dot{w} + W u = 0. \quad (1)$$

For the controlled cabin dynamics, state-space formulas will be derived next. To this end, first let

$$x = \begin{bmatrix} x_S \\ \dot{x}_S \end{bmatrix}$$

denote the state vector and assume that the chassis displacement vector  $w$  is the output of the linear-shape filter

$$\dot{x}_w = A_w x_w + B_w \vartheta, \quad (2)$$

$$w = C_w x_w$$

with  $A_w \in R^{n_w + n_w}$  and  $\vartheta \in R^4$  where  $\vartheta$  shows white-noise road excitations. Further, assume that the filter  $(A_w, B_w, C_w, 0)$  has a zero at  $s = \infty$  with multiplicity at least two. This assumption is not stringent and, for example, is satisfied by the vehicle system under consideration. The relative degree assumption implies that  $C_w B_w = 0$ . Hence,

$$\ddot{x}_S = -M^{-1} [K S \quad C S \quad - (K C_w + C C_w A_w)] x_a - M^{-1} W u,$$

where

$$x_a = \begin{bmatrix} x \\ x_w \end{bmatrix}.$$

Then,

$$\dot{x}_a = A x_a + B_1 \vartheta + B_2 u \quad (3)$$

where  $0_{n \times m}$  and  $I_n$  are respectively the  $n$  by  $m$  null and the  $n$  by  $n$  identity matrices and

$$A = \begin{bmatrix} 0_{3 \times 3} & I_3 & 0_{3 \times n_w} \\ -M^{-1}KS & -M^{-1}CS & -M^{-1}(KC_w + CC_wA_w) \\ 0_{n_w \times 3} & 0_{n_w \times 3} & A_w \end{bmatrix}$$

$$B_1 = \begin{bmatrix} 0_{3 \times 4} \\ 0_{3 \times 4} \\ B_w \end{bmatrix}, \quad B_2 = - \begin{bmatrix} 0_{3 \times 4} \\ M^{-1}W \\ 0_{n_w \times 4} \end{bmatrix}.$$

The filter parameters  $A_w$ ,  $B_w$ ,  $C_w$  can be identified from the vertical acceleration measurements at the chassis points  $A'$ ,  $B'$ ,  $C'$ ,  $D'$  which constitute the common measurement set used in practice. The identification algorithms developed in (Akçay and Türkay, 2004) and (Akçay, 2011) directly identify transfer function matrices in the state-space form from power spectral density measurements. Alternatively, it can be derived approximately by using first principles. This approach requires a simple bounce model of the truck and will be illustrated in the sequel.

For the controller design, assume that the vertical acceleration and the secondary suspension stroke measurements at the corners  $a$ ,  $b$ ,  $c$ ,  $d$  stacked into the output vector

$$y = \begin{bmatrix} \ddot{z}_S \\ \dot{z}_S \end{bmatrix} = C_2 x_a + D_{22} u, \quad (4)$$

where

$$C_2 = C_{21} C_{22},$$

$$C_{21} = \begin{bmatrix} SM^{-1} & 0_{4 \times 4} \\ 0_{4 \times 3} & I_4 \end{bmatrix}$$

$$C_{22} = \begin{bmatrix} -KS & -CS & (KC_w + CC_wA_w) \\ S & 0_{4 \times 3} & -C_w \end{bmatrix},$$

$$D_{22} = - \begin{bmatrix} SM^{-1}W \\ 0_{4 \times 4} \end{bmatrix},$$

are available. From Table 1 and Equation (1), the natural frequencies of the heave, the pitch, and the roll motions of the cabin are computed 1.6145, 1.2761, and 1.8493 Hertz, respectively. The damping ratios of these modes are respectively 0.1552, 0.1144, and 0.0981. The significance of these values, in particular the natural frequencies will be emphasized later.

The twelve-degrees of freedom truck model is assumed to travel with a constant forward velocity along a road profile. A simplified bounce model of the truck is used to study the 'heave-only' motion of the vehicle in Akçay and Türkay (2009). The shape-filter parameters in Equation (2) are obtained by using this model. It is assumed that the displacement excitations at the chassis points  $A'$ ,  $B'$ ,  $C'$ ,  $D'$  are independent. This assumption may be hardly justifiable; but guarantees the simultaneous excitation of all the three body motions of the truck cabin. The derivative of the road

roughness, i.e.,  $\zeta$  is commonly specified as a random variable  $\mu\sqrt{v}\eta(t)$  where  $v$  is the vehicle's forward velocity,  $\mu$  is the road roughness coefficient, and  $\eta(t)$  is a unit intensity white-noise process. In this study,  $v$  and  $\mu$  are fixed as  $v = 20$  m/s and  $\mu = 0.0027$ . Thus, the covariance function of  $\zeta$  denoted by  $R_\zeta$  satisfies

$$R_\zeta(\tau) = \mu^2 v \delta(\tau)$$

where  $\delta(\tau)$  is the unit impulse function.

### 3. MULTI-OBJECTIVE CONTROL VIA FIXED ORDER OPTIMIZATION

In this section we consider the following multi-objective control design problem. Before, let's make the following arrangements; Stack the heave, the pitch and the roll accelerations of the cabin into a vector  $r_{21} = [\ddot{z}_G \quad \ddot{\theta} \quad \ddot{\phi}]^T$ , and the suspension travels into a vector  $r_{22} = \dot{z}_S$ , and let  $T_{r_{21}\eta}(s)$  and  $T_{r_{22}\eta}(s)$  denote the closed-loop transfer functions from  $\eta$  to  $r_{21}$  and  $r_{22}$ . For a given transfer function matrix  $T(s)$  analytic on the open right-half plane, let  $\|T\|_\infty$  denote its  $H_\infty$  norm. (See, for example Zhou (1996)). Recall that when a system with scalar transfer function  $T(s)$  is driven by a unit intensity white-noise input, its  $H_\infty$  norm has the interpretation as the rms gain of the system. The multi-objective control design problem of this section can be formulated as follows:

*Problem 4.3: Given two matrices  $\Lambda_1$ ,  $\Lambda_2$ , and a number  $\beta_1 > 0$  and a specified controller order  $n_K$ , find an output-feedback controller  $u = K(s)y$  internally stabilizing the closed-loop system and minimizing  $\|\Lambda_1 T_{r_{21}\eta}\|_\infty$  while satisfying  $\|\Lambda_2 T_{r_{22}\eta}\|_\infty < \beta_1$ .*

This is a non-convex and non-smooth optimization problem solved by using the HIFOO toolbox Gümüşsoy et al (2009) when  $n_K$  is less than the order of the passive suspension system. The optimization algorithms in the HIFOO toolbox attempt to find the fixed-order controllers minimizing the closed-loop  $H_\infty$  norm, but do not attempt to find the global minimum. Thus, their success depends on the proper initialization. However, they have been applied with success to various benchmark control design problems in the literature. The authors compared their results with other published design techniques Gümüşsoy et al (2009).

The weight matrices and the parameters are chosen as follows. After some trial and error, we set  $\beta_1=1.1$  and let  $\Lambda_1^{-1} = \text{diag}(\|G_{\ddot{z}_G\eta}\|_\infty, \|G_{\ddot{\theta}\eta}\|_\infty, \|G_{\ddot{\phi}\eta}\|_\infty)$  and  $\Lambda_2^{-1} = \|G_{\dot{z}_S\eta}\|_\infty I_4$ . These are empirical values and the optimal values for the weight matrices or the parameter  $\beta_1$  will not be searched.

In Table 2, the rms response variables are displayed for the passive and the active suspensions for controller orders varying from zero to six designed by the HIFOO toolbox. The vertical accelerations and the suspension travels at the four corners of the truck cabin are used as the measurement signals for the system. Interestingly, the controllers of low orders achieve best performances. Surprisingly, a static gain controller provides a very good performance recruitment in comparison to the other order controllers even with the quarter-car active suspension designs. The simulation results displayed in Table 2 for the zeroth order HIFOO design show that the rms heave, pitch and roll accelerations are decreased by 60.31%, 73.82% and 66.38%, respectively, while the rms suspension travels are only increased by about 5.26%, and the rms gain of the suspension travels remain almost unchanged.

Table 2. The rms responses of the passively and actively suspended cabin model with HIFOO controllers of order  $n_K$ .

rms	Passive	$n_K: 0$	$n_K: 1$	$n_K: 3$	$n_K: 6$
$\ T_{\ddot{z}_{G\eta}}\ _2$	0.710	0.281	0.278	0.221	0.232
$\ T_{\ddot{\theta}_\eta}\ _2$	0.595	0.155	0.217	0.106	0.117
$\ T_{\ddot{\phi}_\eta}\ _2$	1.338	0.450	0.407	0.362	0.430
$\ T_{r_{22}\eta}\ _2$	0.038	0.040	0.040	0.040	0.042
$\ T_{r_{22}\eta}\ _\infty$	0.134	0.135	0.134	0.134	0.135

Figures 2-4 show the magnitudes of the heave, the pitch and the roll accelerations of the truck cabin to the warp input for the passive suspension and the HIFOO design for  $n_K = 0$ . Once more it is acknowledged that the designed active suspension suppresses the body vibrations without increasing the suspension travels. The rms values of  $u_A, u_B, u_C, u_D$  computed as 293.5, 364.9, 220.1, and 185.9 respectively, show that the actuator saturation is not likely to happen.

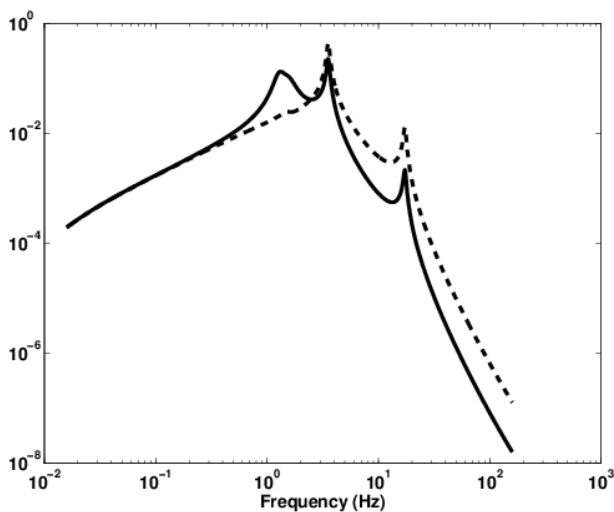


Fig. 2. The heave acceleration frequency response magnitudes of the passive suspension and the HIFOO design

for  $n_K = 0$  to the warp input  $\gamma(t)$ : (-) passive suspension, (- -) active suspension.

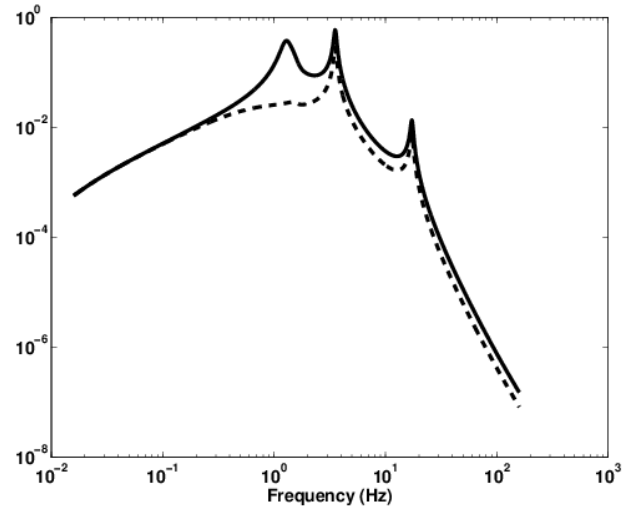


Fig. 3. The pitch acceleration frequency response magnitudes of the passive suspension and the HIFOO design for  $n_K = 0$  to the warp input  $\gamma(t)$ : (-) passive suspension, (- -) active suspension

The performance enhancement by the HIFOO designs is remarkable in comparison to the controllers designed in Akçay and Türkay (2009). It has been observed that the HIFOO controller of order 3 outperforms the full order Linear Quadratic Gaussian controller designs in Akçay and Türkay (2009). The HIFOO design for a static or first order controller is even better than the reduced order LQG controller. For comparison the stochastic responses of the truck cabin for the third order reduced LQG and the HIFOO controllers are given in Table 3.

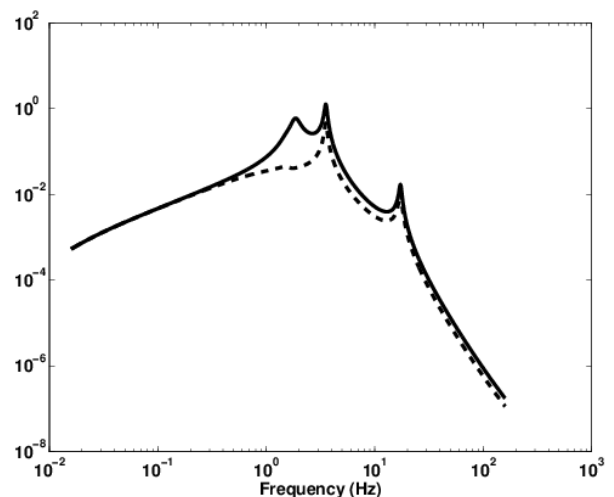


Fig. 4. The roll acceleration frequency response magnitudes of the passive suspension and the HIFOO design for  $n_K = 0$  to the warp input  $\gamma(t)$  at corner A: (-) passive suspension, (- -) active suspension.

Table 3. The rms responses of the passive suspension, the 3th order reduced order LQG design truncation and the 3th order HIFOO design.

rms	Passive	LQG	HIFOO
$\ T_{\ddot{z}_G\eta}\ _2$	0.7102	0.5729	0.2215
$\ T_{\ddot{\theta}\eta}\ _2$	0.5950	0.4746	0.1061
$\ T_{\ddot{\phi}\eta}\ _2$	1.3389	0.9832	0.3629
$\ T_{r_{22}\eta}\ _2$	0.0380	0.0356	0.0400
$\ T_{r_{22}\eta}\ _\infty$	0.1347	0.1353	0.1342

Impressively, the rms accelerations of the heave, the pitch and the roll motions are decreased by 68.81%, 82.17% and 72.90% for the HIFOO designs as opposed to 19.33%, 20.24% and 26.57% decreases for the reduced order LQG designs. The rms suspension travels are decreased by 6.32% for the reduced order LQG design and they are increased by about 5.26% for the HIFOO design. The rms gain of the suspension travels remain almost unchanged for both designs. It is seen that the performance of the HIFOO is excellent in comparison to the LQG controller. The simulation results demonstrate that the HIFOO paradigm is as an effective alternative to the existing LQG control design methodology. Moreover, the HIFOO paradigm is more flexible in that it allows the designer to set the controller order *a priori*.

#### 4. CONCLUSIONS

In this paper, a three-degrees-of-freedom cabin ride model of a commercial truck was developed for an active/semi-active suspension application. A simplified bounce model of the truck is used to relate the road excitations at the wheels to the derived from to the accelerometer readings of the chassis at the cabin suspension attachment points can be obtained by using. Then, the multi-objective suspension control problem was formulated as a non-convex and non-smooth optimization problem with the controller order constrained to be less than the vehicle model order. Controllers of various orders were synthesized by using the recently developed optimization algorithms in the HIFOO toolbox. Performance enhancement better than that of an LQG design was obtained with a third order HIFOO controllers. Based on this study, multi-objective control of the truck-cabin suspensions via the fixed-order optimization as implemented by the HIFOO toolbox presents a promising alternative to the LQG control methodologies. The experimental test on real trucks remains a future work.

#### REFERENCES

- Thompson, A. G. (1970-1971). Design of active suspensions. *Proc. Ins. Mech. Engineers*, Volume 185, pp. 553-563.
- Hrovat, D. (1993). Application of optimal control to advanced automotive suspension design. *Trans. ASME, J. Dyn. Sys. Meas., Cont.*, Volume 115, pp.328-342.
- Fialho, I. and Balas, G.J (2002). Road adaptive suspension design using linear parameter varying gain scheduling. *IEEE Trans. Contr. Sys. Tech.*, Volume 10, pp.43-54.
- El Madany, M. M. (1988). Stochastic optimal control of highway tractors with active suspensions. *Vehicle System Dynamics*, Volume 17, pp.193-210.
- Tong, R. T., Amirouche, F. and Palkovics, L. (1999). Ride control-a two state suspension design for cabs and seats. *Vehicle System Dynamics*. Supplement, Volume 33, pp. 578-589.
- Gümüşsoy, S., Henrion, D., Millstone M., and Overton, M. L. (2009). Multiobjective robust control with HIFOO 2.0. In: *Proc. IFAC Symposium on Robust Control Design*, Haifa, Israel.
- Overton, M. L. (2011). HIFOO-H-Infinity Fixed Order Optimization: Matlab Package for Fixed-Order Controllerdesign, <<http://www.cs.nyu.edu/overton/software/hifoo>>. [Accessed 2011].
- Akçay, H. and Türkay, S. (2009). Active suspension design for an ideliazed truck cabin. In: *Proc. Europ. Contr. Conf.*, Budapest, Hungary.
- Akçay, H. and Türkay, S. (2011). Influence of tire damping on actively controlled quarter-car suspensions. *Trans. ASME, Journal of Vibration and Acoustics*, Volume 133, p. 054501.
- Uffelmann, F. (1993). Truck development trends in ride behavior. *SAE Trans*. Paper 933010, pp. 910-920.